Electronic Supplementary Information (ESI): Controlling the Morphology of Microgels by Ionic Stimuli

S1 Analysis of the density profile with Model-dependent Mie scattering approach

As described in the main text, we aim to correlate experimentally obtained scattering profiles to radially varying density profiles within the particles. While Rayleigh-Gans-Debye (RGD) theory can be applied to correlate the scattering of the laser light in the sample to the radial distribution of refractive index within the particles, the RGD approximation applies to particles of sufficiently small size, as well as limited difference in refractive index with the solvent;

$$|1 - n/n_\mathrm{s}| \ll 1; \tag{1}$$

$$2kR|1 - n/n_\mathrm{s}| \ll 1, \tag{2}$$

where n_s and n are the refractive index of the solvent and the particle, respectively, and $k = 2\pi n_\mathrm{s}/\lambda$ is the wave vector of the incident light that has a wave length λ. Since the microgels in our work have a considerable diameter w.r.t. the wavelength of the laser light, small deviations from the RGD approximation may arise. In light of some of the surprising findings in this work (i.e. the observation of an inverted density profile), therefore, a Mie-theory approach is included to analyze the light scattering of the particles. As we will see, nonetheless, calculated deviations from the RGD model will be very minor, as the difference in refractive index between the hydrogel and the solvent remains small due to significant water uptake. We assume that the relative polymer density profiles in the microgels to be of the expanded form

$$\rho(r) = \tilde{\rho} \left(1 - \frac{r^3}{R_0^3}\right)^{\alpha_0} \prod_{j=1}^{j_\mathrm{max}} (1 + \alpha_j \cos(j\pi r/R_0)), \tag{3}$$

where r is the radial coordinate, while $R_0 > 0$, $0 \leq \alpha_0 \leq 2$, and $-1 \leq \alpha_j \leq 1$ for $j \geq 1$ are the free parameters in this density profile. The scaling factor $\tilde{\rho} = \frac{4}{3}\pi R_\mathrm{p}^3 / \left(\int_{r_0}^{R} 4\pi r^2 \rho(r)\mathrm{d}r \right)$ is included to ensure that the total amount of polymer is conserved. This (dry) polymer mass is set to equal that of a dense sphere ($\rho = 1$) of radius $R_\mathrm{p} \approx 180$ nm, and is determined *via* the hydrodynamic radius of the first sample in the collapsed state at $50°$, which is 213 nm, in combination with an estimated remaining water content of 40%, based on work on macroscopic gels by Hirotsu.[2] Yet, even larger water contents in the collapsed state may be expected. Regardless of $\tilde{\rho}$, Eq. (3) reduces to the theoretically derived density profile for neutral particles as in Ref. [7] for the case $\alpha_0 = 3/5$ and $\alpha_j = 0$ for $j \geq 1$. The density profiles in Eq. (3) can, therefore, be regarded as a perturbation on the earlier derived profile.

The relation between the effective refractive index $n(r)$ at any polymer density $\rho(r)$ can be established using multiple methods, yet the assumption of a linear relationship between these suffices in accuracy for all practical purposes in our case. We employ

$$n(r) = \rho(r)n_{r_p} + (1 - \rho(r))n_s, \tag{4}$$

in which the refractive indices $n_\mathrm{p} = 1.52$ for pure NIPAM and $n_\mathrm{s} = 1.334$ for water are used. Note that we ignore the imaginary part of the refractive index, as its magnitude may be expected to be too small to be of any effect. Typical values of $n(r) \sim 1.35$ are found for the densest polymer region, which agrees with previous estimates [38] of reasonable values for microgels. We apply the algorithm developed by Pena-Rodriguez *et al.* [29] to calculate Mie-scattering curves from the resulting $n(r)$ directly. After the scattering curves are obtained, 3.8% of the mirrored scattered intensity is added to account for the contribution from the scattered light which is reflected at the air/glass interface at the opposite side of the decaline vat. The strength of this backscattering contribution is based on their known indices of refraction. Finally, polydispersity in the system is included by repeating the Mie-scattering calculations for a range in particle sizes. The full scattering curve, which represents a system with a Gaussian distribution of particle radii, can now be constructed by summing over the weighted contributions from every radius.

By using the reduced weighted chi-square method to quantify the similarity between the resulting numerical and experimental intensity curve, we simultaneously fit R, polydispersity, and α_k to the experimental data. Choosing $k_{\mathrm{max}} = 4$ suffices to yield good correspondence with the experimental data, and this value was consequently used in all fits.

S2 Analysis of density profile with model-independent approach

The data were also analyzed by a free-form method, which is similar to the Gaussian deconvolution approach, [32] adapted to spherically symmetric particles. The structure was taken as consisting of N concentric shells, where the radius of the shells were, respectively, $R_n = n/R_{\mathrm{max}}/N$, for $n = 0, 1, \ldots, N$, where R_{max} is the outer radius of the particle. The scattering is then expressed as $I(q) = |A(q)^2|$ where q is the modulus of the scattering vector and the amplitude is

$$A(q) = \left[a(N)V(R_N)\Phi(qR_N) + \sum_{n=1}^{N-1} \left(a(N-n) - a(N-n+1) \right) V(R_{N-n})\Phi(qR_{N-n}) \right] \times \exp\left(-\sigma^2 q^2/2\right).$$ (5)

In this:

$$\Phi(x) = \frac{3\left(\sin(x) - x\cos(x)\right)}{x^3},$$ (6)

$V(R) = \frac{4\pi}{3}R^3$, $\frac{R_{\mathrm{max}}}{4N}$, and $a(n)$ are fit parameters. The Gaussian factor is included to have Gaussian-like shapes of the shells rather than box-like shells. Polydispersity of the particles were included by having a Gaussian number size distribution of R_{max}. In the analysis, 10 shells were used, however, such a large number results in some numerical instabilities and therefore a term is added to the reduced weighted chi-square, χ^2, so that the functional to minimize is

$$L = \chi^2 + \alpha \sum_{n=2}^{N} \left(a(n) - a(n-1) \right)^2,$$ (7)

where α is chosen from a discrepancy criteria so that there is about 10% increase in χ^2 compared to the lowest values. Note that additional restraint biases the solutions in direction of a constant radial density. Back scattering was included in the modelling, with a scale factor, which was also optimized in the fit. The implementation of the

optimization was similar to that described by Pedersen and Hamley. [31]

S3   Extraction of density profiles using the model-independent approach

Figure shows the fits to the SLS data for the four different samples described in the main text, using both methods described above. It can be observed that the model-dependent Mie-scattering method and the model-independent approach both produce satisfying fits. We therefore proceed by comparing the resulting density profiles, as shown in Fig S2. It is found that the model-independent approach reproduces the characteristic inverted density profile, i.e. a decreased density in the core of the microgel, although the effect seems to be slightly smaller in three out of four samples. In general, good agreement on the density profiles may be observed, and when the mass distribution is considered in Fig S2 (e-h), the correspondence is even better. We observe that due to the nature of the model-indepedent approach, a sharp particle surface will not be defined easily, which is merely a practical consideration here. We find a slightly larger outward movement of mass in the Fig S2 (g-h), suggesting that deprotonation could have an even slightly larger effect on the core swelling. Given these results, we are confident that our conclusions regarding the density profile and the distribution of mass are robust and reproducible.
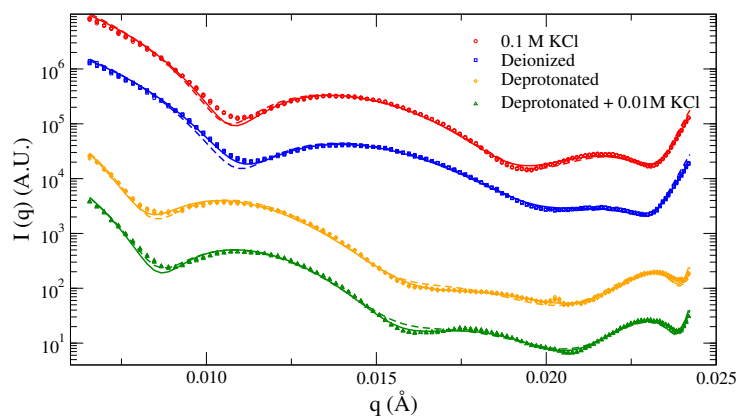
Figure S1: Fitted form factors using the model-independent approach (full curves), as well as the model-dependent Mie-scattering approach (dashed). Also the experimental data points are shown. The data has been shifted to show results for all four samples in one figure.
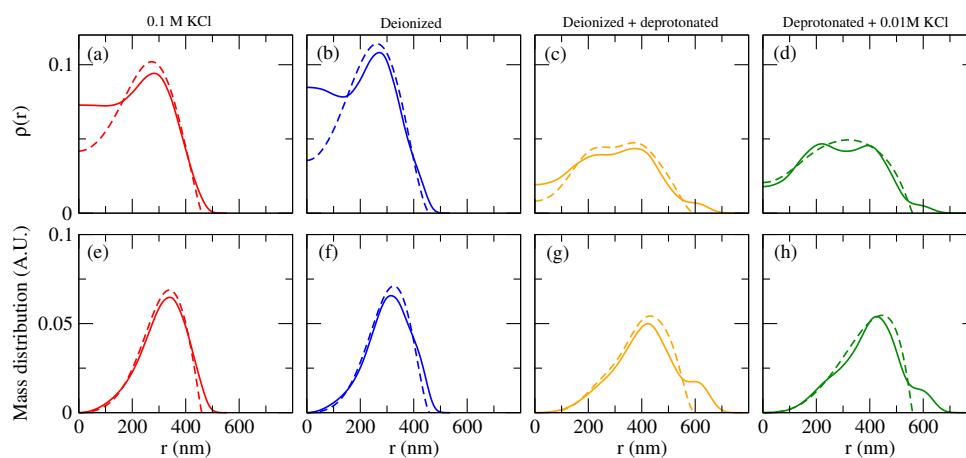
Figure S2: The calculated density profiles (a-d), as well as the radial mass distribution $4\pi r^2 \rho(r)$ in (e-h). The dashed curves are obtained using the model-independent approach (full curves), while the approach based on the model-dependent Mie scattering is shown by the dashed curves.